

ICAS-90-6.3.3

**ON THE DEVELOPMENT OF THE BAFR  
(BASIC AIRCRAFT FOR FLIGHT RESEARCH) IN PORTUGAL**

*by L.M.B.C. Campos and J.R.C. Azinheira*

Instituto Superior Técnico, 1096 Lisboa Codex, Portugal  
Work supported by JNICT and also by CAUTL/INIC

**Abstract**

*This paper describes briefly (§2) the development in Portugal of the BAFR (Basic Aircraft for Flight Research), which is a CASA 212 Aviocar twin-turboprop light transport of the Portuguese Air Force, fitted with an extensive set of instrumentation offered by the N.L.R., and a telemetry system given by the D.L.R., as part of a data acquisition and processing system designed at the Aeronautics Laboratory of IST at Lisbon Technical University. The paper also outlines two research projects making direct use of this flight test facility; (§3) the establishment of a severity scale for the magnitude of atmospheric disturbances, in terms of their effect on aircraft flight performance; (§4) validation of a non-linear model of the longitudinal stability of an aircraft in a dive, allowing a determination of time and lengthscales for a stabilized or steady flight regime to be attained, from any given initial condition. The introduction (§1) indicates the circumstances which made possible the development of a flight test capability in Portugal, and the conclusions (§5) suggests its possible uses at national and international level.*

**1. Introduction**

There are few countries in the world which have dedicated flight test aircraft, usually operated by large aeronautical research establishments, in support of a major aerospace industry, which is a significant component of the national economy and/or an important contributor to exports. Examples include a variety of flight test aircraft operated by NASA (National Aeronautics and Space Administration) and FTCs (Flight Test Centers) of the armed forces in the USA; RAE (Royal Aircraft Establishment), AAEF (Armament and Aeroplane Experimental Establishment) and RSRE (Royal Signals and Radar Establishment) in the U.K., the C.E.V.s (Centres d'Essais en Vol) at Brétigny, Istres and Cazaux in France, the D.L.R. (Deutsche Luft und Raumfahrt) and EP61 (Eprobungstelle 61) in Germany, N.L.R. (National Luft und Ruimtevaart Laboratorium) in the Netherlands, R.S.V. (Riparto Sperimentale di Volo) in Italy, and N.A.E. (National Aerospace Establishment) in Canada, to which should be added flight test aircraft operated by the USSR. It may seem surprising that such a distinguished short list could be joined, even in modest terms, by a small country, which does not

occupy a central role in aeronautical research, design and production; it is the purpose of the present paper to explain how the development of an independent flight test capability in Portugal has been possible, since this may be a worthwhile example to follow in the enlargement of the international aerospace community.

The recent (1988-90) development of a flight test capability in Portugal was made possible by a combination of factors: (i) the role of AGARD (Advisory Group for Aerospace Research and Development) as an international forum through which major offers of equivalent were channelled to Portugal, viz. flight test instrumentation from the N.L.R. in Amsterdam, and telemetry equipment from D.L.R. in Braunschweig, as well as training of technicians, at Braunschweig Technical University; (ii) the cooperation at national level between the Portuguese Air Force, which made available the CASA 212 Aviocar Aircraft, and the Aeronautics Laboratory at the Instituto Superior Técnico (Engineering Faculty) of Lisbon Technical University, which designed the installation and managed the programme; (iii) the existence in the country of a long tradition of aircraft operations and maintenance, making possible that all aircraft modifications be carried out at OGMA (Oficinas Gerais de Material Aeronáutico) in Alverca, and flight test operations conducted from the AFA (Air Force Academy) at Sintra Air Base, the locations being 25 km from Lisbon, respectively to the North and the West; (iv) the support of Portuguese and European community research and formation programmes, namely the funding of JNICT (National Board for Scientific and Technological Research) under its programme for Research Infrastructure, and the training of technicians on instrumentation under the PEDIP (Specific Programme for the Development of Portuguese Industry) programme of the European Community (EC). The CASA 212 Aviocar operates in a dual role configuration: (i) the sensors and flight test instrumentation do not interfere with the continuation of the use of the aircraft for aerial photography and survey; (ii) fitting equipments rack in the cabin and a 4-meter instrumentation boom over the nose converts the aircraft in a few hours to the flight test role.

## 2. Elements of LNEV (National Flight Test Laboratory)

The development of an independent flight test capability in Portugal was made possible by the offer made by the NLR (National Aerospace Laboratory) in Amsterdam, through the FMP (Flight Mechanics Panel) of AGARD [1], to transfer to Portugal free of charge, a large set of flight test instrumentation, worth US\$0.7 million when new. This instrumentation was used in the civil Fokker F.27 Friendship and F.28 Fellowship Airliners and in the military Dutch-Canadian NF-5 version of the Northrop Freedom Fighter, and had been superseded by new equipment intended for the Fokker 50 turboprop and 100 turboprop-powered airlines and the Dutch version of the General Dynamics F-16 Fighting Falcon.

The instrumentation was transported from Amsterdam to Lisbon in a Portuguese Air Force C-130 Hercules Aircraft, and then transferred to the Aeronautics Laboratory at the Instituto Superior Técnico of Lisbon Technical University. There was enough instrumentation to keep a considerable backlog of spares, after setting-up a complete ground bench simulating the instrumentation system in the aircraft, as well as setting aside the instruments for the latter. The Aeronautics Laboratory was set-up with funds from the Research Infrastructure Programme of JNICT (National Board for Scientific and Technological Research), and belongs to the Modeling Group at IST which designed the installation.

The programme has been managed under a Memorandum of Understanding (MoU) signed by the chief-of-staff of the Portuguese Air Force and the rector of Technical University; the MoU covers cooperation in research and training in several areas, but was actually motivated in the first instance by the flight test facility. Under the memorandum the Portuguese Air Force makes available a CASA 212 Aviocar (see Figure 1), which is quite suitable as a BAFR (Basic Aircraft for Flight Research), due to the long endurance and low cost of operation of its twin turboprop propulsion system, and the generous volume and payload which can be accommodated in the fuselage.

The IST (Instituto Superior Técnico), where is located the Aeronautics Laboratory, is an engineering school with 6000 students, 1000 teaching and 600 support staff, which awards diplomas, M.Sc. and Ph.D. degrees in most technical disciplines (Mechanical, Electrical, Civil, Chemical, Materials and Mining Engineering, plus Mathematics and Physics), but not in Aeronautics. Some members of the Modeling Group, originally Mechanical or Electrical Engineers, received 3 months of general training on flight test techniques at the Institut für Flugführung of Braunschweig Technical University, which operates its own

Dornier 28 and 128 test aircraft, as well as a Do 228 of the German Antarctic survey. This was followed by several weeks of specialized training at N.L.R. in Amsterdam, on the instrumentation offered to Portugal.

The instrumentation system for the aircraft (Figure 2) was designed at the Aeronautics Laboratory, and receive signals from a variety of sensors (Table 1). The detailed installation drawings and work were performed at OGMA (Oficinas Gerais de Material Aeronáutico) in Alverca, 25 km north of Lisbon. OGMA is a major aircraft repair and modification facility, employing 2700, and occupying 116.000 m<sup>2</sup> covered area, at their own airfield, which has a 3-km runway, on the banks of the estuary of the river Tagus, upstream of Lisbon. These tasks were well within the capabilities of OGMA, which regularly performs major repair and overhaul on aircraft, engines and systems (e.g. C-130/L-100 Hercules, A-7 Corsair II, Dassault Falcon, etc...), and produces airframe components (for Aerospatiale Puma and Lama helicopters, Dornier 228 and CASA 212 aircraft, etc.), deriving more than 2/3 of its income from foreign customers.

An upgrade of the independent flight test capability came again through AGARD, this time through the FTTWG (Flight Test Techniques Working Group), with the offer of telemetry equipment, including transmitters, receivers, aerials and tape recorder worth US\$0.2 million when new. This equipment operates in the VHF/UHF band, and was used by the D.L.R. at Braunschweig, until interference with other radio emissions on both sides of the then German border dictated changing to equipment using a higher frequency band. As with the earlier transfer of flight test instrumentation from NLR in Amsterdam, and the training of technicians there and at Braunschweig Technical University, AGARD is supporting missions connected with the training of Portuguese technicians at the donor's site in the use of the equipment, and verification visit by technicians from the donor to check installation performed in Portugal.

The CASA 212 Aviocar flight test aircraft belongs to Flight 401, which operates from the air base at Sintra 25 km West of Lisbon, not far from the mountain range of the same name, where the mouth of the Tagus and the Atlantic coast meet. The base also houses the AFA (Air Force Academy), where is located the data processing facility in support of flight tests. It is intended that the ground segment of the telemetry system, including the original helical antennas supplied by the D.L.R., be mounted on a jeep-type all-terrain vehicle, so that telemetry can be used on test flights not only from Sintra but also from other locations. A request has been made under the national investment plan PIDDAC (Plan for Investments in Development) for the facilities in Sintra to be expanded, to

include a self-contained calibration facility for all on-board instrumentation.

The development of a flight test facility involves not only equipment, but also specialized staff. The nucleus of staff has been the Modelling Group at the Aeronautics Laboratory at Lisbon Technical University, but in reality they have been supported by technicians at the DE (Directorate for Electrical Systems) and DMA (Directorate for Mechanics and Materials) at the Air Force Headquarters, at OGMA (the maintenance and production facility) and at AFA (Air Force Academy). Five Air Force Engineers are following a two-year training course and hand-on practice programme, under a PEDIP (Specific Programme for the Development of Portuguese Industry) action with EC (European Community) funds. This course is run at the Aeronautics Laboratory, and will be coordinated with the requirements of an M.Sc. at Lisbon University for three of the Air Force Engineers. The programme has been managed by professors at the University, and is already contributing to another three M.Sc. degrees, involving research on several topics, some of which are discussed below.

### 3. An intensity scale for the severity of atmospheric disturbances

An arbitrary flow velocity  $\vec{v}$  may be decomposed into an uniform stream  $\vec{U}$ , a dilatation represented by the divergence  $\nabla \cdot \vec{v}$ , and vorticity, represented by the curl  $\nabla \wedge \vec{v}$ . An uniform stream corresponds to a force  $F$ , e.g. lift  $L$  or drag  $D$ :

$$F = C_F \frac{1}{2} \rho U^2 c, \quad (1)$$

where  $\rho$  is the mass density,  $c$  the chord for the force per unit span on a wing,  $U$  the free stream velocity, and  $C_F$  the dimensionless force

coefficient. The dilatation  $\nabla \cdot \vec{v}$  is associated with compressibility, e.g. wave drag at supersonic speed, and is negligible at low  $M^2 \ll 1$  Mach number  $M = U/s$ , where  $s$  is the sound speed.

The vortical force is given by:

$$\vec{H} = \rho s \vec{v} \wedge (\nabla \wedge \vec{v}), \quad (2)$$

as the product of the mass density  $\rho$ , by a reference area  $s$ , by Lamb's [2] vector, which is the outer product of the velocity  $\vec{v}$  by the vorticity  $\nabla \wedge \vec{v}$ , and is due to eddies crossing streamlines [3]. In the case of an airfoil in a stream sheared transversely  $\vec{v} = U(z) \vec{e}_x$ , the vortical force is given by:

$$H = C_s \rho c^2 U dU/dz, \quad (3)$$

as the product of the mass density  $\rho$ , by the square of the chord  $c$ , the free stream velocity  $U$  and vorticity  $dU/dz$ , and the dimensionless shear coefficient  $C_s$ .

Comparing say lift, to the vortical force (3) with the same direction (3), we have:

$$H/L = 2(C_s/C_L) N, \quad (4)$$

where  $N$  is the dimensionless shear number:

$$N = (c/U) dU/dz, \quad (4)$$

which compares the vorticity to the velocity divided by the chord. Since the interpretation and magnitude of the vortical force, shear coefficient and shear number are discussed in some detail elsewhere [4], we give here only enough data to judge the importance of the vortical  $H$  relative to the lift  $L$  force in (4).

For a Joukowski airfoil [5] the: (i) lift coefficient is  $C_L = 2\pi\bar{\alpha}$ , where  $\bar{\alpha}$  is the effective angle-of-incidence,  $\bar{\alpha} = \alpha - \alpha_0$ , i.e. the incidence  $\alpha$  two-dimensional relative to the angle of zero lift  $\alpha_0$ ; the shear coefficient is  $C_s = \pi/16$ , and is smaller for three-dimensional bodies, which generate less secondary vorticity, since eddies can be deflected past them, unlike in the two-dimensional case. Thus, for a lift coefficient of about unity  $C_L \sim 1$ , the ratio of vortical to lift force (4) does not exceed  $H/L \leq \pi N/8$ . The largest atmospheric wind changes recorded [6] are 75 m/s over 30 m, corresponding to a vorticity  $dU/dz \sim 2.5 \text{ s}^{-1}$ , and shear number  $N = 0.2$  for a chord  $c = 3$  m and stream velocity  $U = 150$  m/s; in this case  $H \leq 0.01 L$  and the vortical force is negligible compared to lift. Only in the wakes [7] of propellers  $N \sim 5$ , can the vortical force become significant  $H/L \leq 2$ .

The preceding examples show that, with the possible exception of an aircraft flying through the wake of another, lift (and drag) are not affected by atmospheric vorticity per se, and can be calculated from the local flow velocity, e.g. by:

$$L = \frac{1}{2} \rho S C_L U^2, \quad (6)$$

where  $C_L$  is the lift coefficient,  $S$  the reference area of the aeroplane, and  $U$  the groundspeed for flight in still air; in the presence of wind, of longitudinal  $u$  and vertical velocity components  $w$ , respectively, we should replace in (6) groundspeed by airspeed, so that lift changes to:

$$L^* = \frac{1}{2} \rho (C_L - (\partial C_L / \partial \alpha) w / (U+u)) \{ (U+u)^2 + w^2 \}, \quad (7)$$

where we have taken into account that there is a change of incidence  $\Delta\alpha \approx \tan(\Delta\alpha) = w/(U+u)$ , which affects the lift coefficient. The disturbance intensity, defined as the relative lift change:

$$G \equiv L^*/L - 1 = 2 u/U - (\partial C_L / \partial \alpha) w/U, \quad (8)$$

is given by (8) for moderately strong winds  $u^2, w^2 \ll U^2$ , viz. not exceeding 30% of the ground speed.

The disturbance intensity can be determined either from aerodynamic data (4), or from its effects on flight mechanics, as we proceed to show. For steady, straight and level flight, lift balances the weight:

$$W = L = \frac{1}{2} \rho S V^2 C_L(\alpha); \quad (9)$$

in the presence of atmospheric disturbances the airspeed changes to  $V^*$ , the incidence to  $\alpha^*$  and there may be a vertical acceleration  $A$ :

$$W = mA = L^* = \frac{1}{2} \rho S V^* C_L(\alpha^*), \quad (10)$$

where  $m$  is the mass of the aircraft,  $W=mg$  the weight, and  $g$  the acceleration of gravity. The ratio of (10) to (9) is:

$$(1 + A/g) (V/V^*)^2 = C_L(\alpha^*)/C_L(\alpha) \quad (11)$$

where the change in the lift coefficient is due both to the atmospheric disturbance:

$$C_L(\alpha^*) = C_L(\alpha) [1 + G - (\alpha^* - \alpha)/\bar{\alpha}], \quad (12)$$

and to the change of incidence.

From (11) and (12) it follows that the disturbance intensity can be calculated from the vertical acceleration  $A$ , the change of airspeed  $V, V^*$  and the change of incidence  $\alpha, \alpha^*$ , by:

$$G = (1+A/g) (V/V^*)^2 - 1 + (\alpha^* - \alpha)/(\alpha - \alpha_0). \quad (13)$$

For example, for an aircraft flying through the disturbance at constant incidence and airspeed:

$$V^* = V, \alpha^* = \alpha: \quad G = A/g, \quad (14)$$

the disturbance intensity is the vertical acceleration measured in  $g$ 's. Other alternative interpretations are given elsewhere [8]. For an aircraft flying at constant incidence and without vertical acceleration, viz. near the stall:

$$\alpha^* = \alpha, A=0 \quad V_s^* = V_s / \sqrt{1+G}, \quad (15)$$

the stall speed is raised  $V_s^*$  by negative

disturbances  $G < 0$  which cause a lift loss, e.g. a disturbance intensity  $G_1 = -0.17 g$  raises the stall speed  $V_s^* = 1.1 V_s$  to unstick speed, and can cause stall at take-off. Similarly [9], a stall at approach to land  $V_s^* = 1.3 V_s$  can be caused by a lift loss corresponding to a disturbance intensity  $G_2 = -0.42 g$ .

The disturbance intensity can be measured in other flight conditions, e.g. in a steady turn at a bank angle  $\phi$ , the component of lift on the plane of the flight path  $L \sin \phi$ , balances the centrifugal force, equal to mass  $m$  times centrifugal acceleration  $\Gamma$ :

$$(L/m) \sin \phi = \Gamma = V^2/R = \omega^2 R, \quad (16)$$

where  $R$  is the turn radius, and we denote by  $V$  the airspeed and  $\omega$  the instantaneous turn rate. All of these may change in the presence of an atmospheric disturbance.

$$(L/m) (1+G) \sin \phi^* = \Gamma^* = V^{*2}/R^* = \omega^{*2} R^*, \quad (17)$$

so that the disturbance intensity satisfies:

$$(1+G) (\sin \phi^* / \sin \phi) = \Gamma^* / \Gamma = \\ = (V^*/V)^2 R/R^* = (\omega^*/\omega)^2 R^*/R. \quad (18)$$

The main idea is that whereas in a given flight condition, e.g. straight and level (13) or steady turn (18), various flight parameters may change, they do so in an interrelated manner, specifying a disturbance intensity  $G$ , which is a measure of the severity of the atmospheric perturbations found in flight. The correlation of these quantitative measures with subjective ratings can be done in a simulator, or better still, in flight tests.

#### 4 - Non-linear pitch stability in a dive in still air

The preceding theory of flight in a perturbed atmosphere can be extended from performance to stability [10], including simulation of flight in windshears [11]. We choose as a further example of a problem deserving verification through flight testing, what is arguably the simplest non-linear model of longitudinal stability. We consider (Figure 3) an aircraft in a dive with a constant glide slope, starting with an arbitrary initial velocity. We assume that the pitch angle is changed so as to keep the aircraft on the same approach path, and wish to predict how the incidence or speed must vary as a function of time or distance to achieve this. The simplest model decouples lateral from longitudinal motion, and neglects rotational inertia, so that the short period mode is ignored and only the phugoid mode is compensated.

In this case the transverse component of weight balances the lift (9):

$$W \cos \gamma = L = C_L(\alpha) \frac{1}{2} \rho U^2 S, \quad (19)$$

and the longitudinal component adds to drag D in subtracting from thrust T, with the balance equating to the inertia force:

$$T - D - W \sin \gamma = (W/g) dU/dt, \quad (20)$$

which equals the mass  $m=W/g$  times the acceleration along the flight path. Bearing in mind that drag is specified by the same law as lift (19), viz.:

$$D = C_D(\alpha) \frac{1}{2} \rho U^2 S, \quad (21)$$

where  $C_D(\alpha)$  is the drag coefficient, we deduce from (19, 20, 21) a single equation for the velocity:

$$g^{-1} dU/dt = -\sin \gamma + T/W - \cos \gamma C_D/C_L, \quad (22)$$

if thrust T and drag-to-lift ratio are expressed in terms of velocity alone.

For subsonic flight we can neglect wave drag, and the drag coefficient consists of (i) form drag, due to skin friction, which is independent of lift; (ii) induced drag, which is proportional to the square of the lift coefficient; (iii) a non-parabolic correction to the lift-drag, which is proportional to lift:

$$C_D(\alpha) = C_{Df} + k [C_L(\alpha)]^2 + \lambda C_L(\alpha). \quad (23)$$

The last term in (22) can be written:

$$\begin{aligned} \cos \gamma C_D(\alpha) / C_L(\alpha) &= \cos \gamma C_{Df} / C_L(\alpha) + \\ &+ k \cos \gamma C_L(\alpha) + \lambda \cos \gamma = (\rho S / 2W) C_{Df} U^2 + \\ &+ (2W / \rho S) k \cos^2 \gamma U^{-2} + \lambda \cos \gamma, \end{aligned} \quad (24)$$

in terms of the velocity where (23) and (19) were used. We have assumed in (20) that the thrust acts along the flight path, and further we take a thrust-weight ratio:

$$T(U)/W = f_0 - f_1 U^2 - f_2 / U^2, \quad (25)$$

which, apart from a constant term, has a dependence on velocity similar to that of the drag (24).

Substituting (24) and (25) into (22) our non-linear pitch stability model reduces to a single equation for the velocity:

$$g^{-1} dU/dt = a - bU^2 - d/U^2, \quad (26)$$

with three parameters specified by the flight path angle  $\gamma$  and the aerodynamic and propulsion characteristics of the aircraft:

$$a \equiv f_0 - \sin \gamma - \lambda \cos \gamma, \quad (27a)$$

$$b \equiv f_1 + C_{Df}(\rho S / 2W), \quad (27b)$$

$$d \equiv f_2 + k \cos^2 \gamma (2W / \rho S). \quad (27c)$$

The equation balances the acceleration along the flight path, made dimensionless by dividing by the acceleration of gravity, against the dimensionless total longitudinal force on the aircraft.

The equation (26) may be written in the form:

$$g^{-1} dU/dt = -b(U^2 - U_-^2)(U^2 - U_+^2) / U^2, \quad (28)$$

where  $U_{\pm}$  denote the steady flight speeds, for which the acceleration is zero, viz  $dU/dt=0$  for  $U=U_{\pm}$ , where:

$$U_{\pm}^2 = \{a \pm \sqrt{a^2 - 4bd}\} / 2b. \quad (29)$$

The steady flight speeds coincide at the minimum drag speed:

$$\begin{aligned} U_{md} &= a / 2b = \\ &= (f_0 - \sin \gamma - \lambda \cos \gamma) / (f_1 + C_{Df}(\rho S / 2W)); \end{aligned} \quad (30)$$

for constant thrust  $f_1=0$ , level flight  $\gamma=0$ , and symmetric lift-drag polar  $\lambda=0$ , this simplifies to  $U_{md} = f_0 C_{Df} \rho S / 2W$  as it well known [12]. The condition for steady flight to be possible is  $a^2 \leq 4bd$  in (29), and leads by (27a,b,c) to:

$$\begin{aligned} (f_0 - \sin \gamma - \lambda \cos \gamma)^2 &\geq 4 \\ (f_1 + \rho S C_{Df} / 2W) (f_2 + k \cos^2 \gamma 2W / \rho S), \end{aligned} \quad (31)$$

the latter simplifies for level flight  $\gamma=0$ , symmetric polar  $\lambda=0$  and constant thrust  $f_1=0=f_2$ , to the known [12] condition  $f_0 \geq 2 \sqrt{k C_{Df}}$ .

From (28) we can obtain the sign of the acceleration, which may be interpreted in Figure 4: (i) above the upper steady flight speed  $U > U_+$ , thrust is exceeded by drag, mainly form drag (plus the longitudinal component of weight) and thus the aircraft decelerates  $dU/dt < 0$  in (28), towards the upper steady flight speed; (ii) between the two steady flight speeds  $U_- < U < U_+$  there is excess thrust, and the aircraft accelerates  $dU/dt > 0$  in (28), towards the upper steady flight speed, and away from the lower; (iii) below the lower steady speed  $U < U_-$  there is again excess drag (mainly

induced drag due to high incidence), and the aircraft decelerates  $dU/dt < 0$  in (28), away from the lower steady flight speed, and towards the stall. We may check this by integrating (28) in the form:

$$\exp = \{-2bgt(U_+ + U_-)\} =$$

$$\left[ \frac{U(t) - U_+}{U_0 - U_+} \right] \cdot \left[ \frac{U_0 + U_+}{U(t) + U_+} \right]^{1/(1-U_-/U_+)}$$

$$\left[ \frac{U_0 - U_-}{U(t) - U_-} \right] \cdot \left[ \frac{U(t) + U_-}{U_0 + U_-} \right]^{1/(U_+/U_- - 1)} \quad (32)$$

where  $U_0 = U(0)$  is the initial velocity at time  $t=0$ . It follows from (32) that after a long time  $t \rightarrow \infty$ , the velocity either tends to the upper steady flight speed  $U(t) \rightarrow U_+$ , which is stable, or diverges from the lower steady flight speed, which is unstable since  $U(t) - U_-$  increases with  $t$ .

Instead of having time as a function of velocity in (32), we could have distance along the flight path  $\xi$ , by writing the acceleration in the form:

$$dU/dt = (dU/d\xi) (d\xi/dt) = U dU/d\xi =$$

$$= \frac{1}{2} d(U^2)/d\xi, \quad (33)$$

substituting in (28) and integrating. For flight away from the stall, the lift coefficient  $C_L \sim \alpha$  is proportional to the effective incidence  $\alpha \sim 1/U^2$ , which is proportional to the inverse square of velocity. Thus we may relate time  $t$  or distance along the flight path  $\xi$ , to incidence  $\alpha$ , viz. through:

$$\exp(-2bg\xi) = \left[ \frac{1/\alpha(\xi) - 1/\alpha_+}{1/\alpha_0 - 1/\alpha_+} \right]^{1/(1-\alpha_+/\alpha_-)}$$

$$\left[ \frac{1/\alpha_0 - 1/\alpha_-}{1/\alpha_0 - 1/\alpha_+} \right]^{1/(\alpha_-/\alpha_+ - 1)} \quad (34)$$

where  $\alpha(\xi)$  is the incidence at position  $\xi$  along the flight path,  $\alpha_0 = \alpha(0)$  the initial incidence, and  $\alpha_{\pm}$  the incidences for steady flight. Again as distance increases  $\xi \rightarrow \infty$  the aircraft tends to the stable flight incidence  $\alpha(\xi) \rightarrow \alpha_+$ , or diverges from the unstable incidence, i.e.  $\alpha(\xi) - \alpha_-$  increases with  $\xi$ . We plot in Figure 5 the velocity divided by the minimum drag speed as a function of dimensionless time:

$$V(X) \equiv U(t)/U_{md}, \quad X = 2bg(U_+ + U_-), \quad (35a,b)$$

and in Figure 6 incidence divided by minimum drag incidence:

$$\Theta(R) \equiv \alpha(\xi)/\alpha_{md}, \quad R \equiv 2bg\xi, \quad (36a,b)$$

as a function of dimensionless distance.

The timescale  $\tau$  and lengthscale  $\ell$  for the motion:

$$1/\ell \equiv 2bg, \quad 1/\tau = (U_+ + U_-)/\ell, \quad (37a,b)$$

are calculated elsewhere [13] and we conclude by interpreting the plots in Figures 5 and 6, as follows: (i) if the initial velocity is above, and incidence below, that for the stable steady flight condition, there is convergence towards the latter; (ii) if the initial velocity, or incidence, lie between the steady flight values, there is convergence towards the stable value, with an inflexion at the minimum drag value; (iii) if the initial velocity lies below, or initial incidence lies above, the unstable 'steady' flight value, there is a rapid divergence towards the stall. As a result of comparisons of plots such as those in Figures 5 and 6, with flight test data, two conclusions may be drawn: (i) that it is too difficult in flight tests to keep a constant glide slope, e.g. using ILS, without lateral deviations, and therefore the theory should be extended to include lateral motion; (ii) that a constant glide slope can be kept without significant lateral motion, so that discrepancies between the model and flight test data may be explained by taking into account the short period mode. It is therefore desirable to look into flight test results before deciding whether (i) or (ii) should be the main directions of further development of the theory.

## 5 - Conclusion

The two examples of fundamental flight given in §3 and §4, use a small fraction of the capabilities of the flight test aircraft described in §2. The CASA 212 Aviocar BAFR (Basic Aircraft for Flight Research) is fitted with (i) a high-standard of commercially available equipment, including Litton LTN-72 inertial navigation system, Rockwell-Collins weather radar, Computing Devices of Canada Doppler radar, Honeywell autopilot, TRT radio altimeter and an instrument landing system, all of which can be operated independently of the instrumentation system and its sensors, which were designed so as not to interfere with the aircraft systems; (ii) the sensors and instrumentation system record a modest number but wide variety of parameters (see Table), including various speeds, aircraft attitude, linear and angular accelerations, positions of control and high-lift surfaces, pilot stick and rudder pedal forces, engine parameters, navigation system data, and strains on specific structural elements, e.g. engine mountings, allowing in-flight measurement of thrust. The aircraft is therefore suitable not only

for basic, fundamental flight research, but also for tests of new airborne equipment and air traffic control procedures, meteorological measurements, teaching of flight test engineers, etc... The know-how acquired in the development of the present general purpose instrumentation system may also be applied to smaller, specific instrumentation packages for other aircraft.

### References

- [1] L.M.B.C. Campos, A.A. Fonseca & H.F. Ramos, 1988, "On the development of a basic flight test capability and some related research projects", *AGARD CP-452*, 28-1 to 26.
- [2] H. Lamb, 1879, *Hydrodynamics*, Cambridge Univ. Press, 6th ed. 1932.
- [3] L.M.B.C. Campos, 1978, "On the emission of sound by an ionized inhomogeneity", *Proc. Roy. Soc. A351*, 65-91.
- [4] L.M.B.C. Campos, 1984, "On the influence of atmospheric disturbances on aircraft aerodynamics", *Aeronautical Journal*, Paper 1085, 257-264.
- [5] L.M. Milne-Thomson, 1958, *Theoretical Aerodynamics*, MacMillan, repr. Dover 1973.
- [6] J. Clodman, F.B. Muller & E.G. Morrissey, 1968, "Wind regime in the lowest one hundred meters, as related to aircraft take-offs and landings", *World Health Organ. Conference*, 28-43.
- [7] R.J. Vidal, 1962, "The influence of two-dimensional stream on airfoil maximum lift", *J. Aerosp. Sci.* 29, 899-904.
- [8] L.M.B.C. Campos, 1986, "On aircraft flight performance in a perturbed atmosphere", *Aeronautical Journal*, Paper 1305, 302-312.
- [9] L.M.B.C. Campos, 1986, "On the disturbance intensity as an indicator of aircraft performance degradation in a perturbed atmosphere", *Int. Conf. Aviation Safety*, Toulouse, 175-190.
- [10] L.M.B.C. Campos, 1989, "On a pitch control law for constant glide slope through windshears", *Aeronautical Journal*, Paper 1559/1, 290-300.
- [11] L.M.B.C. Campos, A.J.N.M. Aguiar & J.R.C. Azinheira, 1989, "A control law for the compensation of the phugoid mode induced by windshears", *AGARD CP-470*, Geilo, 11-1 to 13.
- [12] M.J. Lighthill, 1986, *An informal introduction to fluid mechanics*, Oxford Univ. Press.
- [13] L.M.B.C. Campos & A.J.N.M. Aguiar, 1989, "On the 'inverse phugoid problem' as an instance of non-linear stability in pitch", *Aeronautical Journal*, Paper 1559/1, 241-253.

### Legends for the figures

**Figure 1** - Schematic diagram of the instrumentation fitted to the CASA 212 Aviocar BAFR (Basic Aircraft for Flight Research).

**Figure 2** - Block diagram of the Data Acquisition System (DAS), including the Power Distribution Unit (PDU), Synchro-to-Digital Converter Unit (SDCU), Under-Deck and Main Rack Connector Panels (UDCP1-2 and MRCP), Signal Conditioning Units (SCU1-3), Digital Converter Unit (DCU) and Pulse Code Modulator (PCM).

**Table:** List of 65 parameters measured by the Data Acquisition System aboard the BAFR.

**Figure 3** - Balance of weight  $W$ , drag  $D$ , lift  $L$  and thrust  $T$  for an aircraft on a constant glide slope.

**Figure 4** - Plot of thrust- and drag-to-weight ratio versus velocity for an aircraft in a dive at a flight path angle  $\gamma$ , showing the stable  $U_+$  and unstable  $U_-$  steady flight speeds and the minimum drag speed  $U_{md}$ .

**Figure 5** - Velocity divided by minimum drag speed versus dimensionless time for an aircraft starting a dive at a flight path angle corresponding to a stable steady flight speed 1.2 times the minimum drag speed, and for 15 equally spaced values of the initial velocity.

**Figure 6** - As for figure 5, with incidence divided by minimum drag incidence, plotted as a function of dimensionless distance along the flight path.

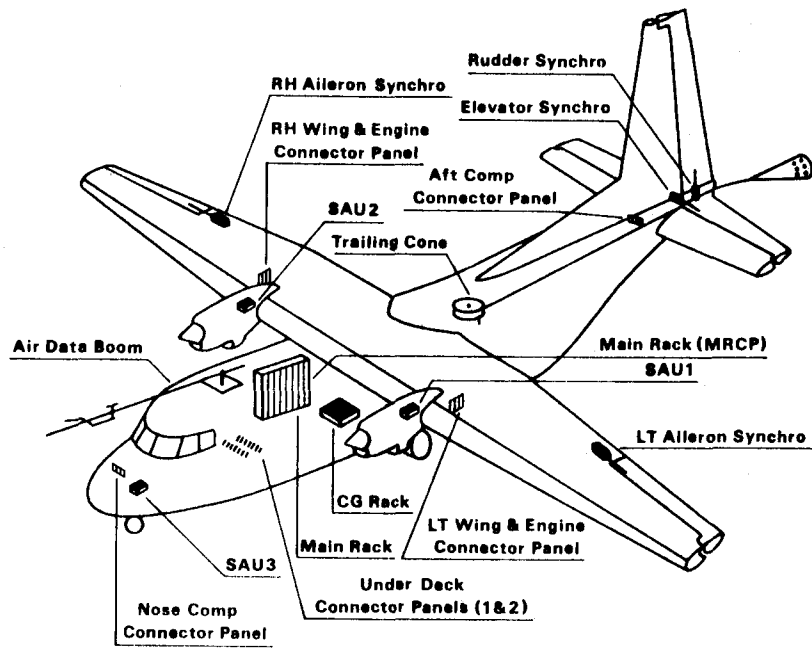


FIGURE 1

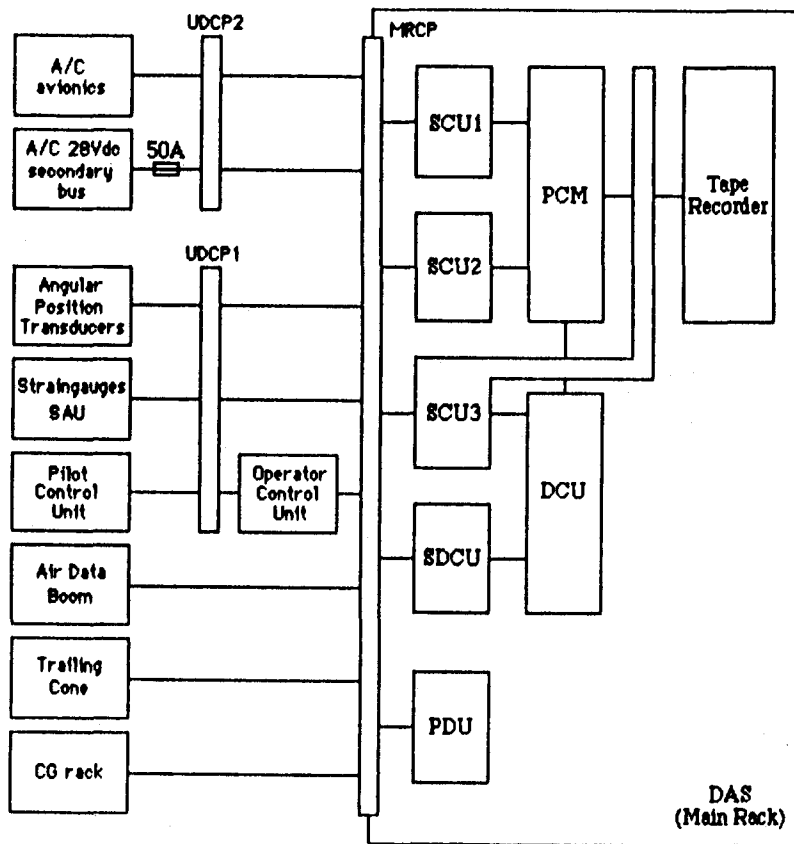


FIGURE 2



Category	Ref	Parameter	Code	Range
General	01	test signal	TS	
	02	time base 1	TB1	
	03	time base 2	TB2	
	04	run counter	RC	1/99
Air Data	05	differential pressure	PD	0/10 kPa
	06	static pressure	PS	30/105 kPa
	07	calibration pressure	PC	0/15 mb
	08	total air temperature	TAT	-50/+50 °C
Configuration	09	ground/flight switch	GFS	on/off
	10	wing flap position	DF	0/45 deg
Control	11	elevator deflection	DE	-30/+20 deg
	12	LT aileron deflection	DA1	-20/+20 deg
	13	RH aileron deflection	DA2	-20/+20 deg
	14	rudder deflection	DR	-25/+25 deg
	15	elevator force	FE	-450/+450 N
	16	aileron force	FA	-300/+300 N
	17	rudder strain A	FR1	
	18	rudder strain B	FR2	
	19	rate of pitch	RP	-20/+20 deg/s
	20	rate of roll	RR	-50/+50 deg/s
	21	rate of yaw	RY	-20/+20 deg/s
	22	acceleration (X-dir)	AX	-1/+1 g
	23	acceleration (Y-dir)	AY	-1/+1 g
	24	acceleration (Z-dir)	AZ	-2.5/+2.5 g
	25	angle of attack	AA	-35/+35 deg
	26	angle of side-slip	AS	-35/+35 deg
	27	angle of pitch	AP	-90/+90 deg
	28	angle of roll	AR	-90/+90 deg
	29	IRS valid signal	IRSf	on/off
Propulsion	30	engine speed L	N1	0/41730 rpm
	31	engine speed R	N2	0/41730 rpm
	32	fuel flow L	FF1	0/1050 lb/h
	33	fuel flow R	FF2	0/1050 lb/h
	34	turbine gas temperature L	TOT1	0/930 °C
	35	turbine gas temperature R	TOT2	0/930 °C
	36	torque pressure L	TP1	0/65 psi
37	torque pressure R	TP2	0/65 psi	
Auto-Flight	38	autopilot engaged	AE	on/off
	39	fight director mode	FDM	1/5
Navigation	40	true heading	HOG	0/360 deg
	41	HOG valid signal	HOGf	on/off
	42	radio altitude	RA	0/7500 ft
	43	RA valid signal	RAf	on/off
	44	localizer deviation	LLD	-90/+90 deg
	45	LLD valid signal	LLDf	on/off
	46	glide slope deviation	GSD	-80/+80 deg
	47	GSD valid signal	GSDf	on/off
	48	drift angle	DFT	-180/+180 deg
49	DFT valid signal	DFTf	on/off	
Thrust	50	A mount strain (L engine)	FA1	
	51	B mount strain (L engine)	FB1	
	52	C mount strain (L engine)	FC1	
	53	D mount strain (L engine)	FD1	
	54	E mount strain (L engine)	FE1	
	55	F mount strain (L engine)	FF1	
	56	G mount strain (L engine)	FG1	
	57	H mount strain (L engine)	FH1	
	58	A mount strain (R engine)	FA2	
	59	B mount strain (R engine)	FB2	
	60	C mount strain (R engine)	FC2	
	61	D mount strain (R engine)	FD2	
	62	E mount strain (R engine)	FE2	
	63	F mount strain (R engine)	FF2	
64	G mount strain (R engine)	FG2		
65	H mount strain (R engine)	FH2		

TABLE I

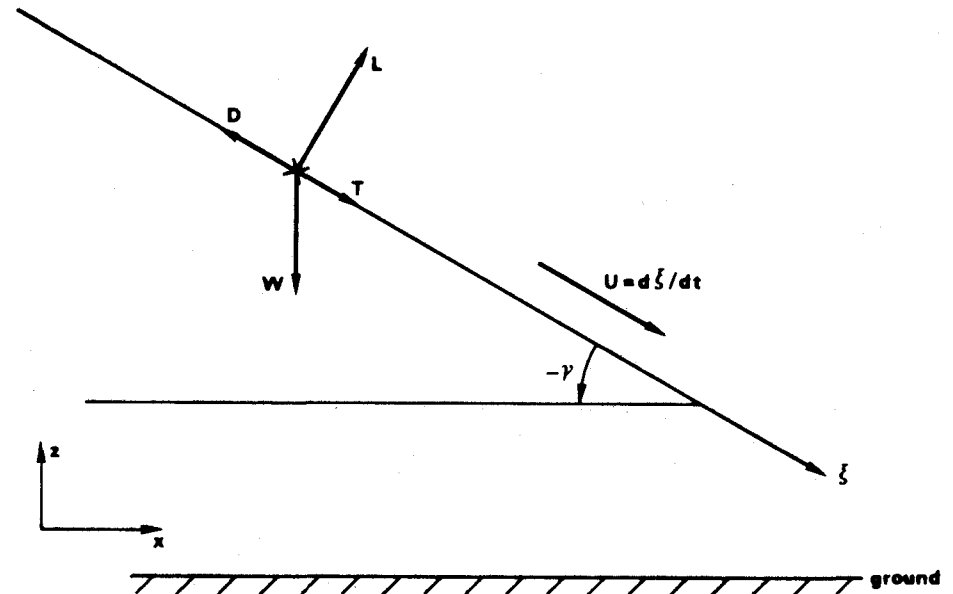


FIGURE 3

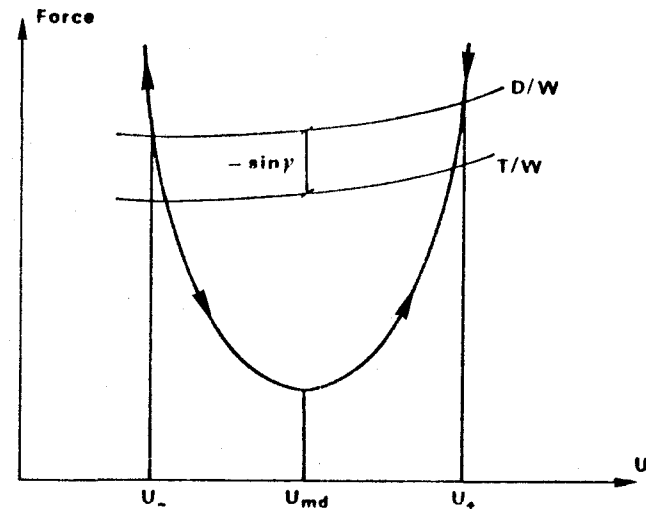


FIGURE 4

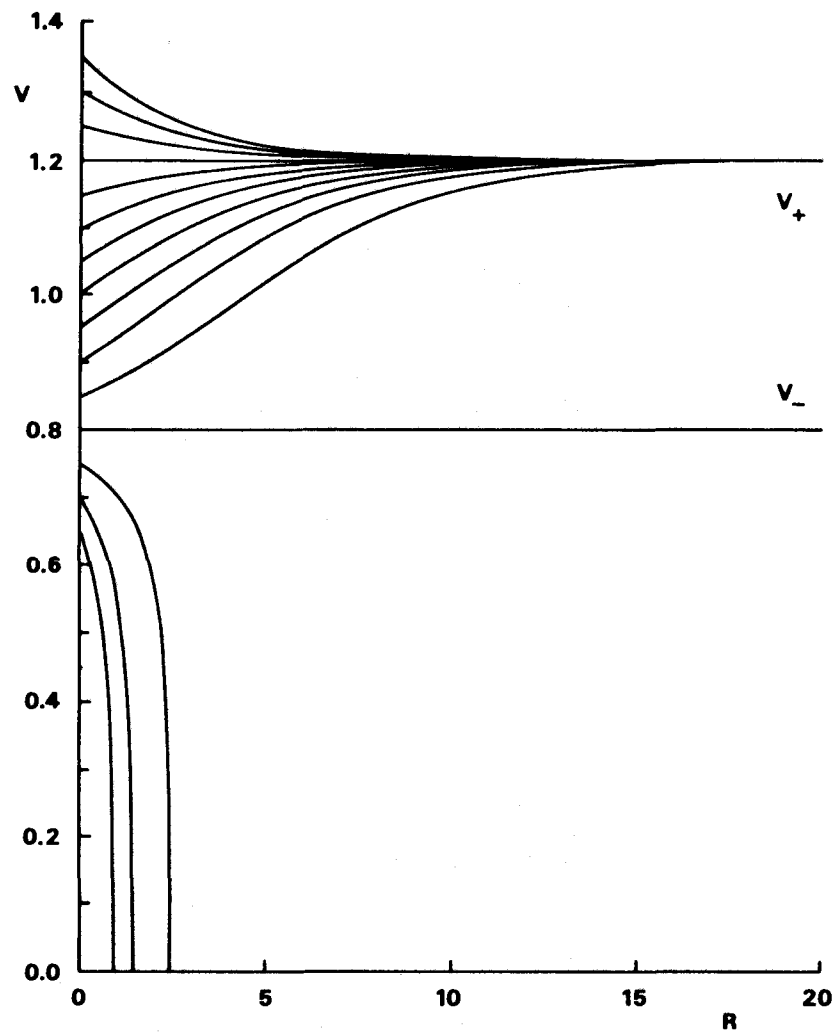


FIGURE 5

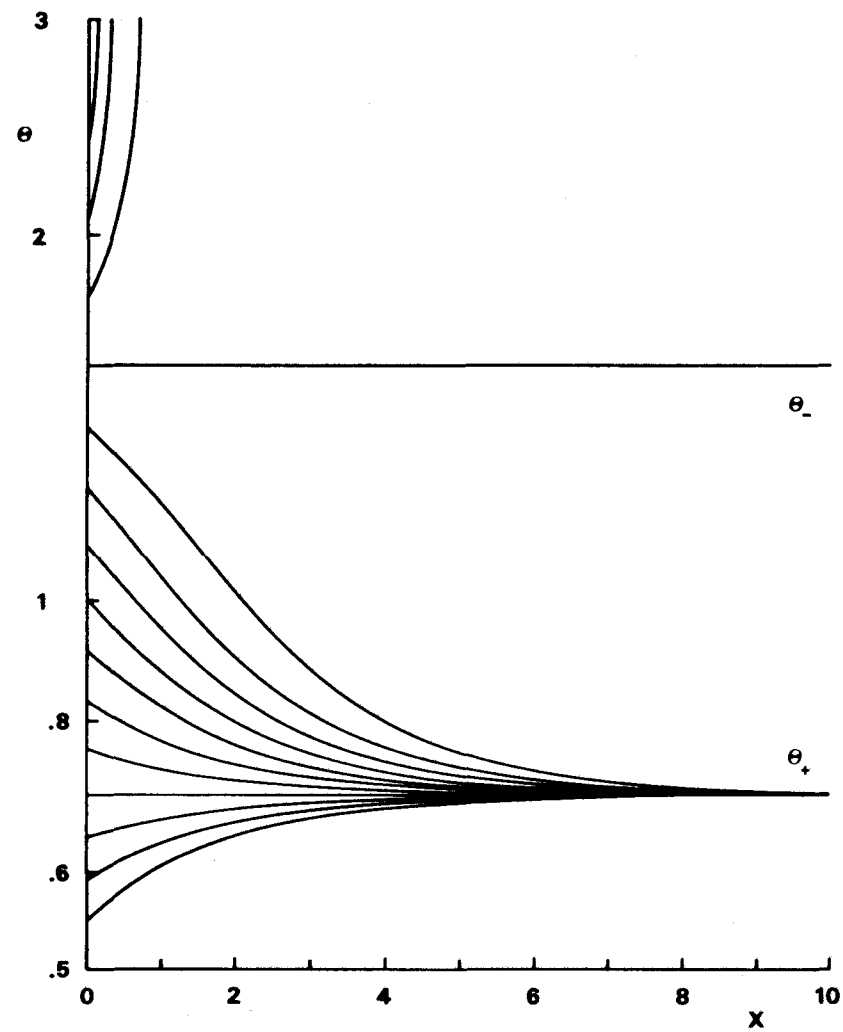


FIGURE 6